Climate Dynamics
https://doi.org/10.1007/s00382-020-05539-1

Assessing changes in the atmospheric water budget as drivers for precipitation change over two CORDEX-CORE domains

Marta Llopart[1] · Leonardo Moreno Domingues[2] · Csaba Torma[3] · Filippo Giorgi[4] · Rosmeri Porfírio da Rocha[2] · Tércio Ambrizzi[2] · Michelle Simões Reboita[5] · Lincoln Muniz Alves[6] · Erika Coppola[4] · Maria Leidinice da Silva[7] · Diego Oliveira de Souza[8]

Received: 2 April 2020 / Accepted: 11 November 2020

Abstract

AQ1

This study evaluates the projected changes in the atmospheric water budget and precipitation under the RCP8.5 scenario over two CORDEX-CORE domains: South America (SAM) and Europe (EUR). An ensemble of five twenty-first century projections with the Regional Climate Model version 4 (RegCM4) and their driving Global Climate Models (GCMs) are analyzed in terms of the atmospheric water budget terms (precipitation, P; evapotranspiration, ET; and moisture flux convergence, C). Special focus is on four subregions: Amazon (AMZ), La Plata basin (LPB), Mid-Europe (ME) and Eastern Europe (EA). The precipitation change signal in SAM presents a dipole pattern, i.e. drier conditions in AMZ and wetter conditions in LPB. Over the two European regions a seasonality is evident, with an increase of ~ 25% in precipitation for DJF and a decrease of ~ 35% in JJA. The atmospheric water budget drivers of precipitation change vary by region and season. For example, in DJF the main drivers are related to the large-scale moisture flux convergence, while in JJA over the AMZ atmospheric moisture flux convergence plays only a minor role and local processes dominate. For JJA in the GCMs the high values of the residual term do not allow us to assess which mechanisms drive the precipitation change signal over the AMZ and LPB, respectively. Same conclusions are found for the RegCM4 JJA simulations over the LPB and EA. This points to the importance of the spatial resolution of climate simulations and the role of parameterization schemes in climate models. Our work illustrates the usefulness of analyzing regional water budgets for a better understanding of precipitation change patterns around our globe.

Keywords Atmospheric water balance · CORDEX-CORE · Climate change · RegCM4

1 Introduction

Changes in precipitation around the globe have been assessed by the Fifth Assessment Report from Intergovernmental Panel on Climate Change (IPCC-AR5 2013). Regional climate studies for South America (SAM; Reboita

Electronic supplementary material The online version of this article (https://doi.org/10.1007/s00382-020-05539-1) contains supplementary material, which is available to authorized users.

✉ Marta Llopart
m.llopart@unesp.br

1 Universidade Estadual Paulista Júlio de Mesquita Filho (UNESP), Bauru, SP, Brazil

2 Departamento de Ciências Atmosféricas, Universidade de São Paulo (USP), São Paulo, SP, Brazil

3 Department of Meteorology, Eötvös Loránd University, Budapest, Hungary

4 Earth System Physics, Abdus Salam International Centre for Theoretical Physics, Trieste, Italy

5 Instituto de Recursos Naturais (IRN), Universidade Federal de Itajubá (UNIFEI), Itajubá, MG, Brazil

6 Centro de Ciência Do Sistema Terrestre, CCST, Instituto Nacional de Pesquisas Espaciais - INPE, São José dos Campos, SP, Brazil

7 Departamento de Ciências Atmosféricas E Climáticas, Centro de Ciência Exatas E da Terra, Universidade Federal Do Rio Grande Do Norte, Natal, RN, Brazil

8 National Centre for Monitoring and Early Warning of Natural Disasters, CEMADEN, São José dos Campos, SP, Brazil

Journal : **Large 382**	Article No : **5539**	Pages : **14**	MS Code : **5539**	Dispatch : **21-11-2020**

et al. 2014a; da Rocha et al. 2014; Llopart et al. 2014, 2020; Chou et al. 2014; Sánchez et al. 2015) and Europe (EUR; Kotlarski et al. 2012; Kovats et al. 2014; Jacob et al. 2014, 2018) have assessed changes in precipitation variability due to global warming and to remote drivers such as the El Niño Southern Oscillation. Although in a warmer world the atmospheric moisture is expected to increase due to enhanced evaporation and water holding capacity (Lu and Cai 2009; Ruscica et al. 2016), precipitation does not linearly respond to these changes (IPCC-AR5 2013). For instance, projections show a strong future drying signal in the eastern portion of the Amazon basin (AMZ) and an increase of precipitation in central Brazil and the La Plata basin (LPB), resulting in a dipolar response of precipitation change over SAM (e.g. Chou et al. 2014; da Rocha et al. 2014; Sánchez et al. 2015; Solman 2016; Llopart et al. 2020). In addition, the precipitation change signal in Europe shows a north–south dipole pattern, more precisely, there is a significant summer precipitation decrease projected over the Mediterranean region and an increase over northern Europe by the end of the twenty-first century (e.g. Giorgi and Lionello 2008; Giorgi and Coppola 2009; Jacob et al. 2014).

Pronounced regional precipitation variability around the world has been associated with local factors (land surface processes, mesoscale drivers: Torma et al. 2015; Ruscica et al. 2016), remote factors (influence of the sea surface temperature from Pacific and Atlantic Oceans: Brönnimann et al. 2007; Llopart et al. 2014) and global climate change (IPCC-AR5 2013; Christensen et al. 2007). One of the tools that can be used to understand what drives the precipitation change signal, is the analysis of the components of the water cycle, which can be separated into an atmospheric and a terrestrial branch. Both branches conserve mass over time, and when the local variation of water storage is negligible, the changes in precipitation may be linked to evapotranspiration, runoff or moisture flux convergence.

In the atmospheric branch of the water cycle, the amount of precipitation can be associated with local feedbacks (e.g. evapotranspiration), remote feedbacks (moisture flux convergence), or both (Nascimento et al. 2016; Furusho-Percot et al. 2019). A few studies analyzed separately the components of the water cycle for present and future climates under different greenhouse gas concentrations (e.g. Mariotti et al. 2011; Dirmeyer et al. 2014; Brêda et al. 2020; Llopart et al. 2020), finding that projected changes in evapotranspiration and precipitation are among the major drivers of the water balance over regions in EUR (e.g. Dezsi et al. 2018) and SAM (e.g. Ruscica et al. 2016; Menéndez et al. 2016; Zaninelli et al. 2019; Llopart et al. 2020).

As Regional Climate Models (RCMs) are increasingly used to downscale Global Climate Models (GCMs) to produce more refined regional climate information (Gutowski et al. 2016; Giorgi 2019), assessing the components of the water balance change signal using both GCMs and RCMs is an important strategy to increase understanding of climate change signals and related uncertainties. Two regions for which such exercise has been carried out are Europe (Dezsi et al. 2018) and South America (Zaninelli et al. 2019; Llopart et al. 2020). The recent completion of a new set of high-resolution dynamically downscaled projections under the CORDEX-CORE (Gutowski et al. 2016) and EURO-CORDEX (Jacob et al. 2014, 2020) initiatives provides the opportunity to revisit the issue of how changes in the water budget affect precipitation projections.

Therefore, the purpose of this study is to assess the precipitation change signal under the RCP8.5 scenario, focusing over two domains from the Coordinated Regional Downscaling Experiment (CORDEX, Giorgi et al. 2009), Europe (EUR) and South America (SAM), and using a new set of projections completed with the Regional Climate Model version 4 (RegCM4, Giorgi et al. 2012) driven by a set of CMIP5 GCMs. Specifically, our aim is to determine the drivers of the projected precipitation changes through the water balance approach and to illustrate the usefulness and limitations of this method.

2 Methodology

2.1 Climate projections

The projections in this study are part of the CORDEX-CORE—Coordinated Output from Regional Evaluations (CORE; Gutowski et al. 2016) experiment, performed with the regional model RegCM4 (Giorgi et al. 2012). For the last three decades the RegCM system has been used for several studies and purposes worldwide (Giorgi 2019).

For the present study, RegCM4 was nested into four GCMs from Coupled Model Intercomparison Project—Phase 5 (CMIP5, Meehl and Bony 2011) over two different CORDEX domains: South America (SAM) and Europe (EUR) (Fig. 1). The GCMs are: Max Planck Institute for Meteorology-Earth system model (MPI-ESM-MR and MPI-ESM-LR; Giorgetta et al. 2012); Hadley Global Environment Model 2-Earth System (HadGEM2-ES; Jones et al. 2011); and Norwegian Earth System Model 1 (NorESM-1 M; Bentsen et al. 2012). HadGEM2-ES was used to drive RegCM4 for both domains, while NorESM-1 M and MPI-ESM-MR only for SAM-22, and MPI-ESM-LR only for EUR-11. In total, we analyze three regional projections for SAM and two for EUR under the RCP8.5 scenario, as summarized in Table 1. Different Representative Concentration Pathways (RCPs, van Vuuren et al. 2011) are available to investigate future climate at continental or regional scales, and the RCP8.5 is

Journal : Large 382 | Article No : 5539 | Pages : 14 | MS Code : 5539 | Dispatch : 21-11-2020

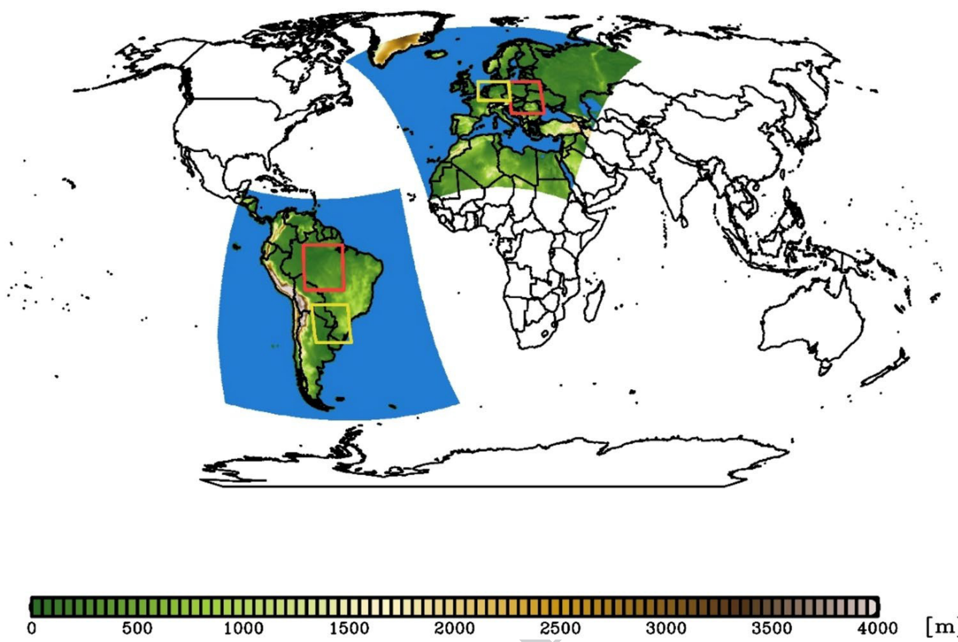

Fig. 1 CORDEX-CORE SAM and EUR domains and topography (shaded, with units in meter). Boxes indicate the subdomains selected for the analysis. LPB (thin yellow box) and AMZ (thick red box) for South America; ME (thin yellow box) and EA (thick red box) for Europe

Table 1 RegCM4 version, horizontal resolution and GCMs forcing used in Europe and South America domains

Domain	Acronym	Horizontal resolution	RegCM4 version	GCM		
				MPI-ESM	HadGEM2-ES	NorESM-1 M
Europe	EUR	0.11°	4.6.1	LR	X	
South America	SAM	0.22°	4.7.0	MR	X	X

LR and MR refer to low and medium resolution, respectively

considered the most extreme one, comprising the highest greenhouse gas concentration by the end of the twenty-first century (corresponding to a radiative forcing of 8.5 W m^{-2}).

RegCM4 is a limited area model that solves the primitive equations in sigma-pressure vertical coordinate and includes different physics parameterization schemes (Giorgi et al. 2012). In this study, RegCM4 was integrated with 25 km (SAM) and 12 km (EUR) horizontal grid spacing and 23 sigma-pressure vertical levels. The simulations cover the period 1970–2100 where the projections refer to the period 2006–2100 (Moss et al. 2010). For both domains, the Community Land Model version 4.5 (CLM4.5; Oleson et al. 2013) is used to represent land-surface processes, whereas cumulus convection is described through a mixed configuration in which the Tiedtke scheme (Tiedtke 1996) is used over land and the Kain-Fritsch scheme (Kain and Fritsch 1990) over ocean. The model configuration for each domain was selected according to preliminary simulations as giving a relatively good performance over the selected domains (Sines et al. 2018; Ciarlo et al. 2018). In order to compare global and regional simulations, as they do not share the same grid or resolution, all data were interpolated onto a regular 0.22° × 0.22° grid (the grid spacing of the majority of the analyzed RegCM4 simulations) using a bilinear method.

2.2 Atmospheric water balance

The hydrological cycle describes the physical processes in which water moves from continental/oceanic surfaces to the atmosphere, and vice-versa, comprising components such as evaporation/transpiration (ET), precipitation (P), surface runoff (R), water storage/transport in the soil and atmosphere. Focusing on a given area, the water balance accounts for water sources and sinks over such region, and it is commonly separated in two branches: the atmospheric and surface balances (Peixoto and Oort 1992; Llopart et al. 2020).

The surface water balance can be expressed as $\frac{\partial S}{\partial t} = P - ET - R$, where $\frac{\partial S}{\partial t}$ is the variation in time of soil water storage (mm day^{-1}) at a given location, which is normally neglected for long term periods. Therefore, on climate time scales the surface water balance can be simplified as: ET = P–R (Peixoto and Oort 1992). In the atmospheric branch, the water balance can be expressed as: $\frac{\partial W}{\partial t} = C + ET - P$, where the first term is the temporal

Journal : Large 382	Article No : 5539	Pages : 14	MS Code : 5539	Dispatch : 21-11-2020

derivative of the precipitable water in a unit area column (mm day^{-1}), and C is the vertically integrated moisture flux convergence (mm day^{-1}). The latter is calculated as$C = -\vec{\nabla}.(\vec{V}q)$, q (g kg^{-1}) and $\vec{V}$ (m s^{-1}) are the air specific humidity and the horizontal wind vector, respectively. Similarly to the surface water balance, for long periods, $\frac{\partial W}{\partial t}$ can be ignored, and thus the atmospheric balance equation can be reduced to P = ET + C (Peixoto and Oort 1992). It follows from this simplification that, over a specific region, P depends on the moisture flux convergence, and on the local evapotranspiration source from the land surface not transported to other regions (Brubaker et al. 1993). The connection between the two branches of the hydrological cycle (surface and atmospheric water balances), when the derivative terms are null, is that C is equal to R.

In this work, we analyze the atmospheric branch of the hydrological cycle. C was integrated in the atmospheric vertical column from the surface to 200 hPa and using time series of daily mean horizontal wind components, specific humidity and surface pressure. The water budget at the global climatological scale is approximately in balance (Brutsaert 2008), but regionally it is often out of balance (Palmer et al. 2008), presenting a residual term due to uncertainties in the model calculations and in the water storage terms. As the global average temperature is projected to increase (IPCC-AR5 2013), specific humidity in the troposphere increases as well, following the Clausius-Clapeyron relationship (Held and Soden 2006), and the storage term from the atmospheric water balance becomes part of the residual term.

The goal of our analysis is to understand the relative roles of land–atmosphere feedbacks (i.e., ET) and large-scale circulation patterns (i.e. C) in determining the regional precipitation change signals over the selected regions.

2.3 Analysis

Although the simulations cover the period 1970–2100, we analyze two time slices: 1995–2014, considered as present climate, and 2080–2100, as far future climate under the RCP8.5 scenario. These periods follow the IPCC recommendation for the AR6 report and the evaluation of the RegCM4 model for present climate over the two domains is given by Ciarlo et al. (2020) and Ashfaq et al. (2020).

Precipitation and wind change signals for December–January–February (DJF) and June–July–August (JJA) are evaluated by comparing the climatology of the far future (2080–2100) with that of the present climate (1995–2014) using ensembles for both GCM and RegCM4 simulations.

In order to attribute the precipitation change signal to large scale versus local/regional forcings, following the methodology of Coppola and Giorgi (2010) and Llopart et al. (2020), we calculated the 20-year running mean anomalies with respect to the reference period (1995–2014) climatology for each atmospheric water balance component (P, ET, C and residual term). Also, we selected two subdomains for each continent as shown in Fig. 1: Amazon (AMZ; 15° S–0°, 65°50° W), La Plata Basin (LPB; 32.5°–20° S, 63°–48.9° W), Mid-Europe (ME; 48.5°–55° N, 2°–16° E) and Eastern Europe (EA; 44°–55° N, 16°–30° E).

The AMZ and LPB are the most important watersheds in SAM. AMZ contains a large area of tropical rainforest while the LPB is the second most extensive basin in SAM and covers parts of five countries. These two basins are connected to each other since the AMZ is one of the moisture sources for LPB via the South America Low Level Jet (SALLJ; Marengo et al. 2004; Drumond et al. 2008).

The ME and EA regions were defined and analyzed during the PRUDENCE project (Christensen and Christensen 2007). They cover fully or partially important European river catchment basins (e.g. Danube and Rhine rivers in ME and Danube and Vistula rivers in EA) and have already been used in several climate studies (Christensen et al. 2008; Giorgi and Lionello 2008; Kotlarski et al. 2012, 2014; Jacob et al. 2018).

3 Results

3.1 Spatial precipitation and wind change signal

Figures 2 and 3 present the GCM and RegCM4 ensemble average changes (2080–2100 minus 1995–2014) in precipitation and horizontal wind components at 850 hPa over the SAM and EUR domains for DJF and JJA, respectively. The 850 hPa is the most representative level of the low-level jet core over the SAM (Montini et al. 2019) and appropriate for similar studies over Europe (Grønås 1995).

Clearly, over both domains, the main broad scale precipitation change patterns are driven by the GCMs and "inherited" by the RCM, however, some significant differences between GCM and RCM patterns are found. Over SAM, for DJF, both the global and RegCM4 ensembles (Fig. 2a, b) show enhanced precipitation along the Intertropical Convergence Zone (ITCZ), with an adjacent decrease in precipitation over its subsidence branch to the north. The trade winds are weakened, as already pointed out in previous studies (Marengo et al. 2012; Reboita et al. 2014a; Llopart et al. 2014; Ambrizzi et al. 2019), so that less moisture enters the Amazon region, which becomes drier than in present climate conditions. The area of reduced precipitation is larger in the RCM than the GCM ensemble, extending in particular over Colombia, Equator and Northern Peru. Over the South Atlantic Ocean, there is an anomalous anticyclonic circulation near south and southeastern Brazil in the GCM ensemble, which is weakly cyclonic in the RegCM4 (Fig. 2a,

Journal : Large 382	Article No : 5539	Pages : 14	MS Code : 5539	Dispatch : 21-11-2020

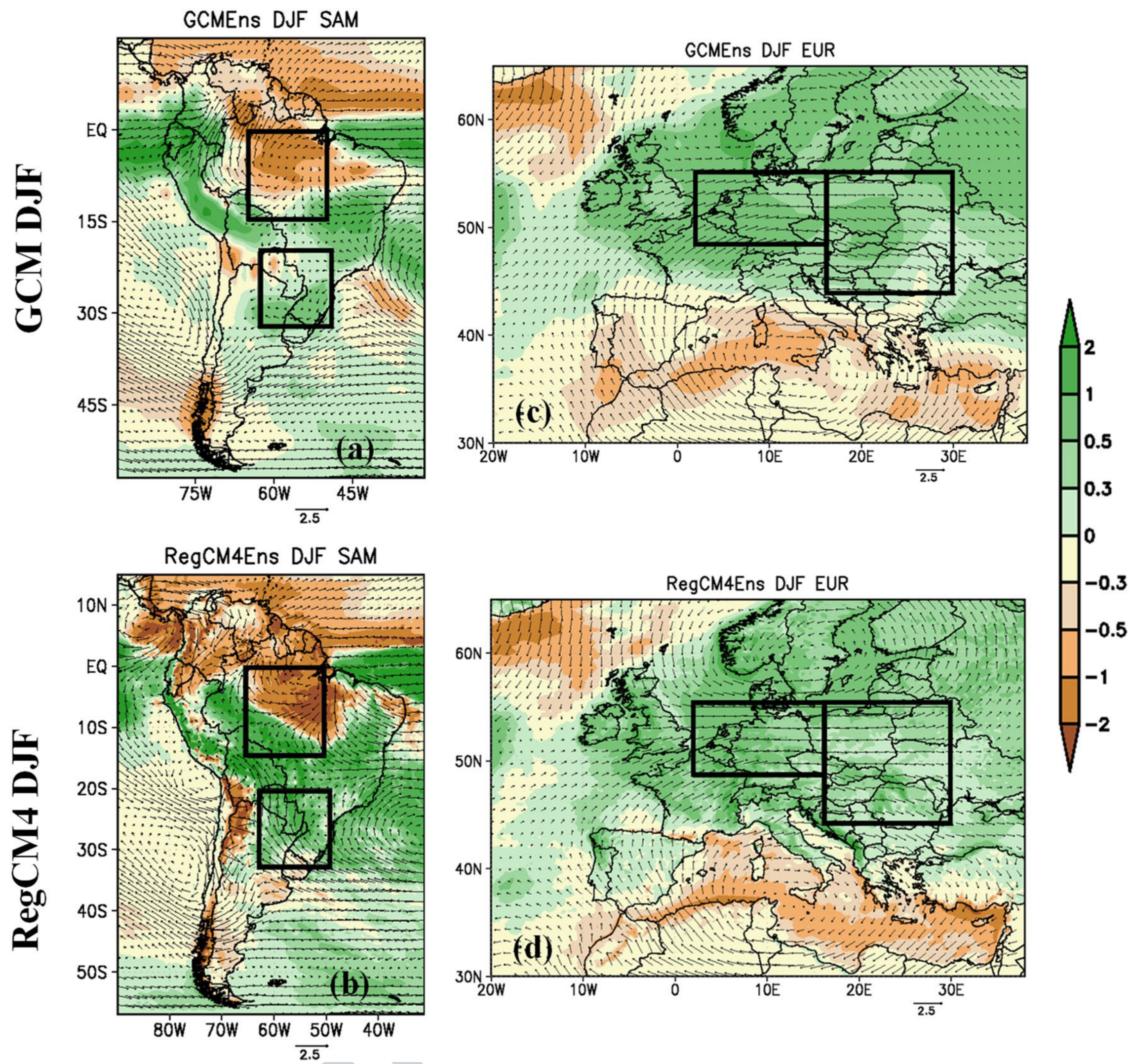

Fig. 2 DJF precipitation (mm day^{-1}) and wind at 850 hPa (ms^{-1}) changes, far future minus reference period, for: **a**, **c** GCM ensemble and **b**, **d** RegCM4 ensemble. SAM is shown left and EUR in the right column. Boxes indicate the subdomains selected for the analysis

b) and results in a more southward extension of the drying area in these regional model projections. However, in both ensembles, there are winds from the ocean to the LPB contributing to moisture supply in this region.

In both ensembles, the SALLJ is weakened and the South Atlantic Convergence Zone (SACZ) is deflected, resulting in a positive anomaly of precipitation in central/eastern Brazil. Moving towards the south, the area of increased precipitation is larger in the RegCM4 ensemble, particularly over Bolivia, Paraguay and southern Brazil. Conversely, the RegCM4 shows an area of reduced precipitation over the LPB, while in the GCMs this reduced precipitation zone is confined to the Atlantic Ocean. Finally, both the RegCM4 and GCM ensembles project reduced precipitation over Southern South America and Northern Chile. In summary, in DJF, both ensembles indicate a precipitation dipole pattern with a precipitation decrease in the Northern regions and an increase in the Central regions of SAM. This feature is basically associated with weaker trade winds and anomalous circulation over the Subtropical South Atlantic. In addition, the signal in the RegCM4 ensemble has greater magnitude than in the GCMs.

The European precipitation change pattern shows the well-known dipole of increased precipitation to the north and decreased to the south, with the transition region of sign reversal moving from about 40° N in DJF to about 60° N in JJA (e.g. Giorgi and Coppola 2007). This pattern is generally followed by the ensembles shown in Fig. 2c, d, however we do find some significant differences between the GCM and RegCM4 patterns. Specifically, during DJF in our simulations we find a positive precipitation change signal in RegCM4 over areas of the Iberian Peninsula, southern

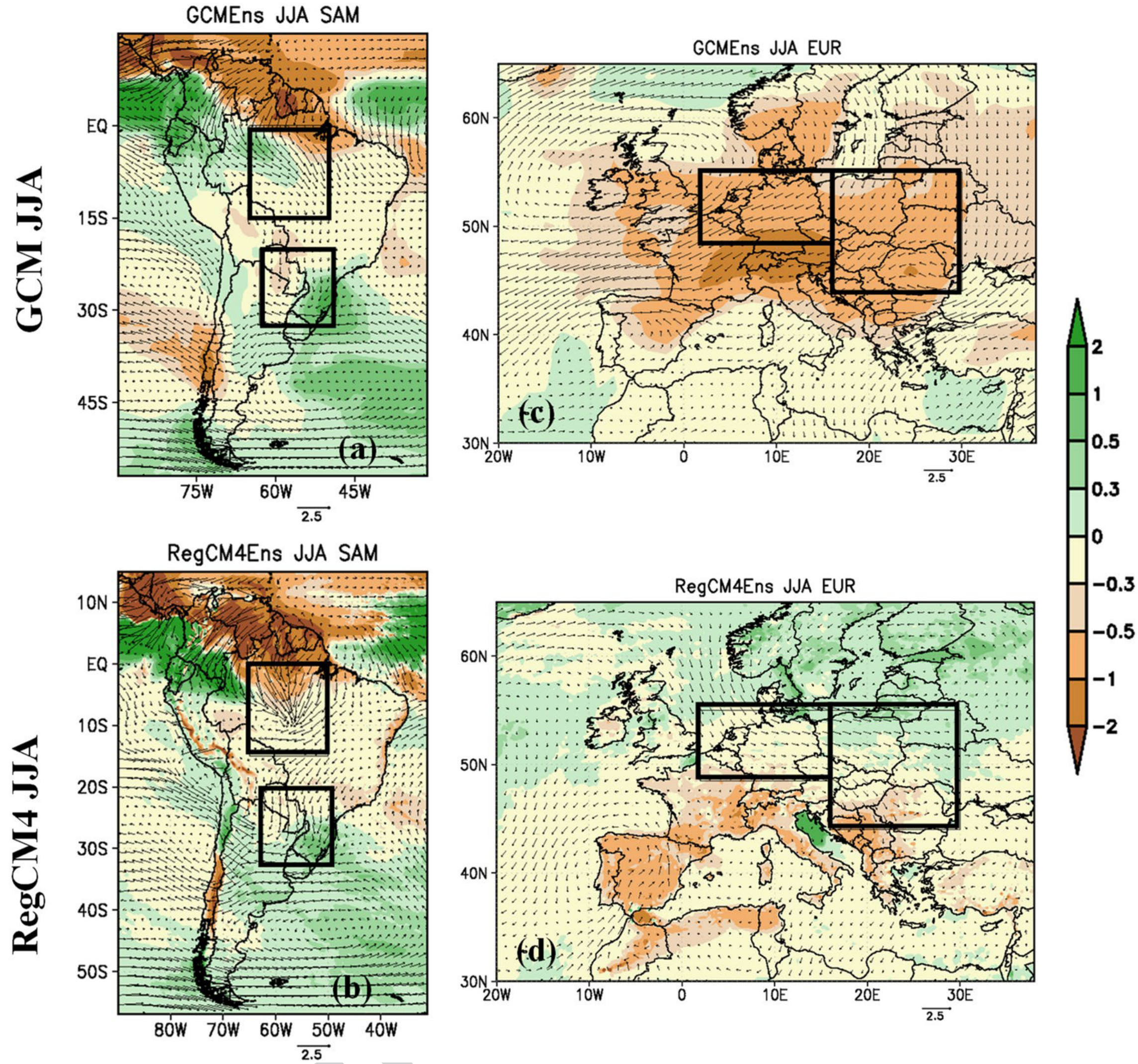

Fig. 3 Similar to Fig. 2, but for JJA

Italy, Greece and southern Turkey for which the GCMs show decreased precipitation. These appear to be associated with the ocean-land mask and topography in the models. In fact, the models project a prevailing decrease of DJF precipitation over the Mediterranean ocean surfaces in response of an enhanced anticyclonic circulation over the Mediterranean Sea. Conversely, the RegCM4 shows increased precipitation over the land areas of the Iberian, Italian and Hellenic peninsulas. This positive signal is thus related to the topographic forcing over these regions, which is not present in the GCMs, whose grid does not capture complex topography and coastline features (Figure S1).

More generally, we note the topographic effect on the precipitation change signal in correspondence of the main mountain chains such as the Alps, Pyrenees and Carpathians (Fig. 2c, d). This signal is mostly of dynamical nature in winter, and it depends on the orientation of the mountain chains (e.g. the Pyrenees or Carpathians) with respect to the prevailing wind changes (Torma and Giorgi 2020). For example, we can see a reduced precipitation signal north of the Pyrenees, in response to the precipitation shadowing effect on the increased southerly winds over the area.

In JJA, the change patterns at the broad scale are generally similar between the GCM and RegCM4 ensembles (Fig. 3), especially in the SAM domain. In the equatorial region, both ensembles (Fig. 3a, b) show a discontinuity of the ITCZ over Northern South America, with a strong precipitation reduction over Venezuela, Colombia and Northern Brazil, and weakly reduced precipitation throughout the Amazon basin, Paraguay and Bolivia, maybe a consequence of transient systems not advancing northward (Blázquez and Solman 2019). In addition, both ensembles show a positive anomaly in Southern Brazil, including the LPB, which may be due to the action of the transient systems in this region

(Blázquez and Solman 2019; Reboita et al. 2020). Again, the magnitude of the signal is greater in the RegCM4 ensemble.

Turning our attention to the European region, most of central to southern Europe experience summer (JJA) drying in both ensembles, but this signal is much more pronounced and more extended in the GCMs (Fig. 3c, d). In fact, in areas of Northern and Northeastern Europe the RegCM4 projects increased precipitation, while the GCM signal is of opposite sign. The general features of the summer precipitation change signal for Europe is consistent with findings of previous analyses (Giorgi and Lionello 2008; Giorgi and Coppola 2009; Jacob et al. 2014, 2020). The reduced area of summer drying in the RegCM4 compared to the driving GCMs, which is consistent across the different members of the ensemble (Figure S2) is not a result specific to this model, but it is common to the EURO-CORDEX ensemble (Jacob et al. 2014; Boé et al. 2020). Boé et al. (2020) attribute it to a number of factors: differences in cloudiness simulations, absence in the RCMs of time varying aerosol concentrations, larger increases in evapotranspiration from the Mediterranean Sea and land areas.

Another important contribution to the different summer precipitation response between GCMs and RegCM is the representation of convective processes at finer resolution (Torma et al. 2015; Giorgi et al. 2016). Figure S3 indeed shows that the precipitation change signal in the RegCM4 has a convective origin. More specifically the RegCM4 simulations indicate a convective precipitation increase over North Europe and decrease over central to southern Europe, while the large-scale precipitation change signal is found to be small (Figure S3). In addition, in summer, topography can strongly modify the precipitation change signal through thermodynamic effects and convection generation induced by high elevation heating (Giorgi et al. 2016; Torma and Giorgi 2020). Therefore, it is likely that a major driver of the differences between GCM and RCM responses is the representation of convection at the respective different resolutions (Figure S1).

Table 2 reports the GCM and RegCM4 precipitation change signal in both seasons over the subdomains shown in Fig. 1. The sign of the regionally averaged change agrees between the two ensembles in all regions, being mostly positive in DJF (except for AMZ) and negative in JJA (except for LPB). The SAM regions show the same change sign in the two seasons, most noticeably consistent drying over AMZ, while the European subregions show a sign reversal. However, as already discussed the magnitude of the change can be quite different between the ensembles, especially in JJA. Specifically, in JJA the RegCM4 indicates stronger drying over AMZ and weaker drying over ME and EA than the GCMs.

Given the precipitation change patterns found in this section, in the next one we will attempt to understand their causes through a water budget analysis.

Table 2 Precipitation changes (%) projected for the end of the century (2080–2100 minus 1995–2014) under RCP8.5 scenario, for DJF and JJA (values in parentheses)

Regions	GCM ensemble	RegCM4 ensemble
AMZ	– 7 (– 14)	– 9 (– 36)
LPB	5 (1)	11 (2)
ME	23 (– 36)	29 (– 7)
EA	21 (– 35)	24 (– 5)

3.2 What drives the precipitation change signal?

In order to understand the driving mechanisms of the regional precipitation signals, we analyze the trends of anomalies (relative to 1995–2014) in the atmospheric water budget components, i.e., precipitation (P), evapotranspiration (ET), moisture flux convergence (C), and the residual term (Res = P-ET-C), estimated for each subdomain of Fig. 1. For each term, we present the box average of global and regional model projections individually, with their respective ensemble average. Average changes of water balance components in Figs. 4 and 5 are summarized in Table 3 for all ensembles, seasons and subdomains and for the present climate and the change (future minus present climate). We also show in the Supplementary Material (Figure S4) the linear regression for each combination of P and ET and P and C (scatter plots and regression fits) components. Slopes of the regression fit are presented in Table 4.

Table 3 shows that in the reference period over most subdomains the residual terms have the same signal in the GCM and RegCM4 ensembles, except over the LPB during DJF and the EA in DJF and JJA. During DJF, we note that ET is the main driving component of the AMZ and LPB precipitation for both the GCM and RegCM4 ensembles, and the residual term is one order of magnitude smaller than the remaining components. On the other hand, the convergence term C drives the precipitation in the European domains, and the residual term is relatively larger with respect to precipitation than in the SAM.

During JJA precipitation in the AMZ and LPB regions is also mostly controlled by ET. The moisture flux divergence acts to reduce precipitation in both the GCM and RegCM4 ensembles over the AMZ, while over the LPB this occurs only in the RegCM4 ensemble. The residual term in JJA is generally similar to the DJF one, except in the GCMs for the LPB (– 1.0 mm day^{-1}). Opposite to the DJF case, in JJA the precipitation in the ME and EA regions is driven by the ET, while moisture flux divergence acts to reduce rainfall in both ensembles.

Journal : Large 382 | Article No : 5539 | Pages : 14 | MS Code : 5539 | Dispatch : 21-11-2020

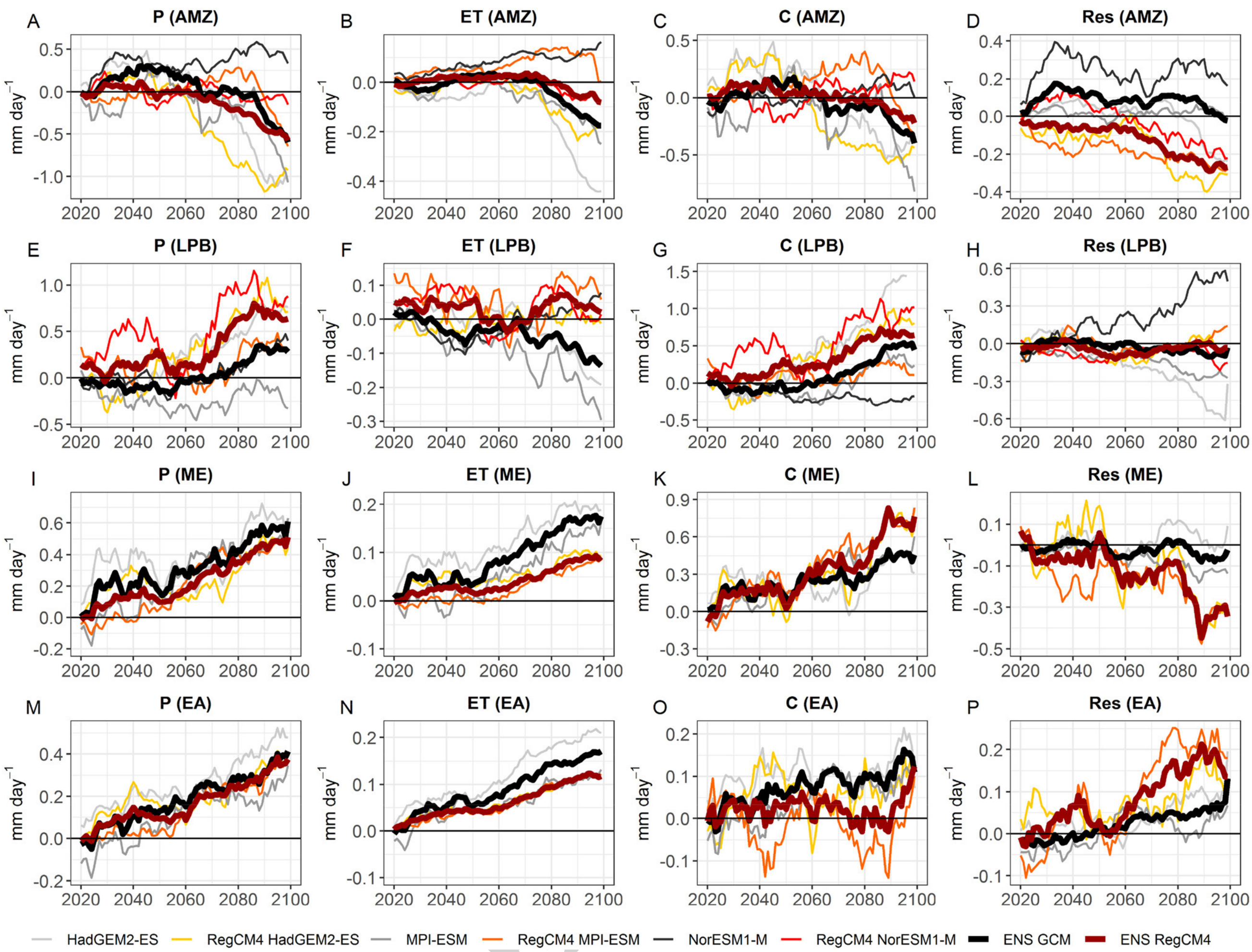

Fig. 4 20-years moving average of anomalies of precipitation (P), evapotranspiration (ET), moisture flux convergence (C) and the residual term (P-ET-C), in mm day^{-1}, from 1995 to 2100, for each individual GCM and RegCM4 and ensemble mean, for DJF in: **a**–**d** AMZ, **e**–**h** LPB, **i**–**l** ME and **m**–**p** EA. The black (red) line represents the GCM (RegCM4) ensemble mean

Figure 4 shows the trends of the regional water budget components in DJF. Most projections indicate an increase in precipitation for AMZ until ~ 2060 (Fig. 4a), of higher magnitude in GCMs, due especially to an increase of moisture flux convergence in the basin (Fig. 4c). After the mid-century, however, there is a reversal in the trend, with all projections indicating a decrease in precipitation until the end of 2100, except NorESM1-M. Precipitation negative anomalies are especially high in HadGEM2-ES and RegCM4 HadGEM2-ES, with decreases of ~ 1 mm day^{-1} by 2100, and in this case, the RegCM4 is strongly dependent on the driving GCM. The pattern of anomalies of moisture flux convergence essentially follows the precipitation pattern in both the global and regional projections, with prevailing positive anomalies in the first half of the century and negative ones in the second half until 2100. Similarly, the evapotranspiration remains roughly constant for the first half of the century and then slightly decreases, evidently in response to the reduced precipitation. We note that the residual term (Fig. 4d) is not necessarily null over the years, probably due to the increased water holding capacity of atmosphere, which makes the assumption of $\frac{\partial W}{\partial t} = 0$ not strictly valid. However, the changes in precipitation and moisture flux convergence projected for the end of the century (Table 3) are around − 0.5 mm day^{-1} and − 0.4 to − 0.3 mm day^{-1}, respectively, and higher in magnitude than the changes in the residual term (~ 0.1 to − 0.2 mm day^{-1}). Therefore, the moisture flux convergence stands as the main driver of the precipitation reduction in global and regional projections at the end of the century, as a response to the weaker trade winds (Fig. 2a, b). Note that the difference in changes between P and C (Table 4) is higher than between P and ET for both global and regional ensembles, especially in the GCM (0.58, against 0.30 in RegCM4). Therefore, the reduced ET in the same period would be a result of the decreased P.

Journal : **Large 382**	Article No : **5539**	Pages : **14**	MS Code : **5539**	Dispatch : **21-11-2020**

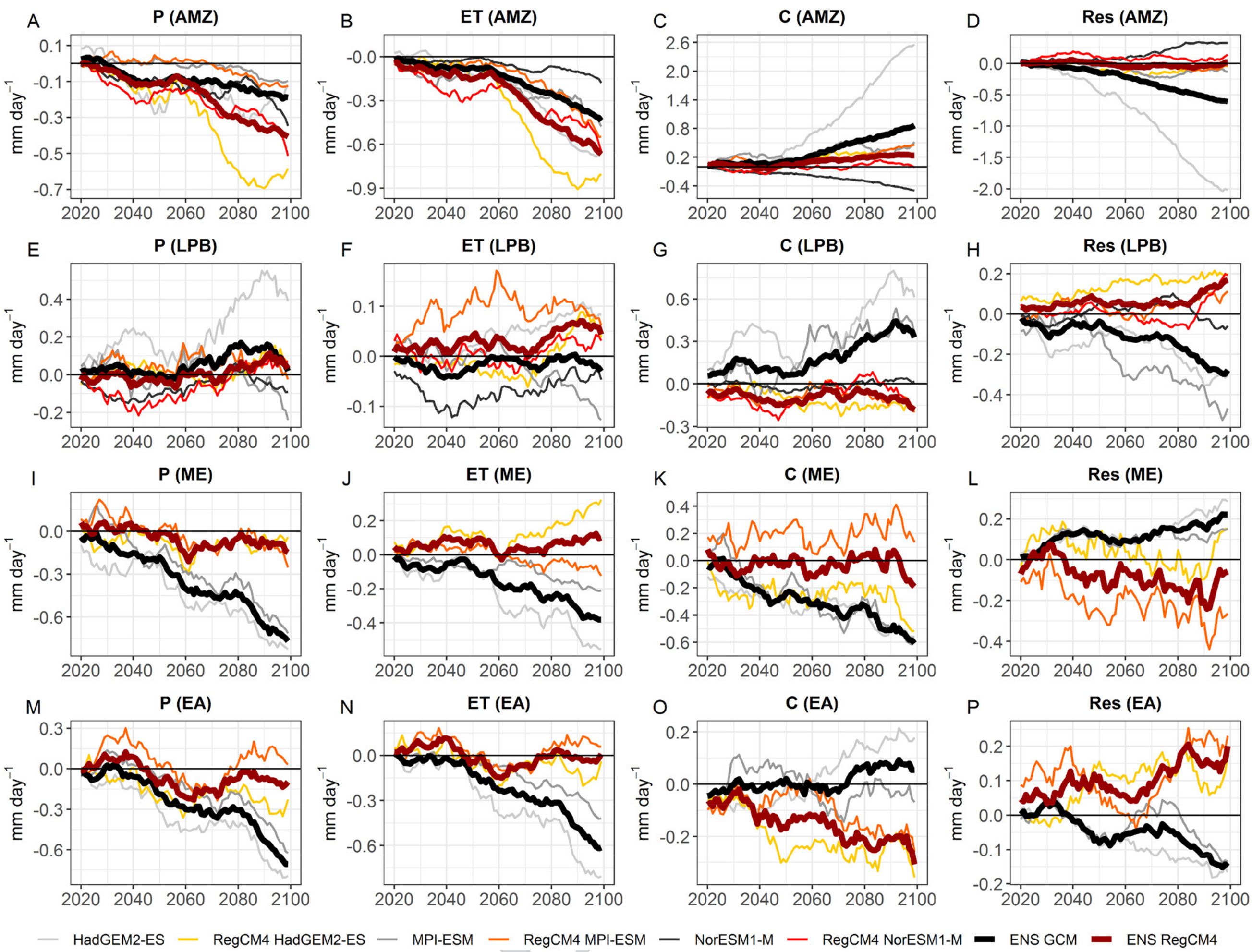

Fig. 5 Similar to Fig. 4, but for JJA

In the LPB during DJF there is a considerable spread between the projections until ~ 2055 (Fig. 4e), with the regional ensemble projecting increasing precipitation and the global ones the opposite. During this period, the precipitation change signal in both ensembles is driven by ET and C (Figs. 4f, g). After 2055, an increase in precipitation is noted in all projections, except MPI-ESM-MR, driven especially by the moisture flux convergence (see the high slopes in Table 4), due to the anomalous cyclonic circulation shown in Fig. 2a, b. The regional ensemble projects a greater increase in precipitation than the global one due to the higher contribution of ET and C. We note that the residual term is close to zero in both the global and regional ensembles (Fig. 4h). In the global ensemble the small residual is due to large contributions of the individual ensemble members of opposite signals, whereas in the regional one the residual is small for each ensemble members. Similarly to the AMZ, for the LPB the changes in moisture flux convergence are higher than the residual term (Table 3) and are driving the precipitation change signal at the end of the century. Interestingly, in the GCM ensemble the ET decreases in the late twenty-first century even though precipitation increases, which implies an increase in runoff or water storage to balance the surface water cycle. The LPB is within a strong hotspot area for land-surface feedbacks and these projections support the findings from Ruscica et al. (2016), which propose the disappearance or a weakening of this hotspot region in the future.

Both the global and regional ensembles project a clear increasing trend in DJF precipitation over the two selected European subdomains (Fig. 4 l, m). Following precipitation, ET has an increasing trend as well, with higher values in the GCMs (Fig. 4j–n). Conversely, the moisture flux convergence shows an irregular behavior, particularly in the EA region, where an increase of moisture flux convergence is clear only in the latter part of the century, while large oscillations are found prior to the last decade of the twenty-first century in the RegCM4 ensemble (Fig. 4o). At the same time, a clear positive trend of moisture flux convergence during the second half of the century in the RegCM4 simulations is more pronounced than in the driving GCM

Table 3 Water balance components [P: precipitation. ET: evapotranspiration. C: moisture flux convergence] over the subdomains for the reference period (1995–2014) and the trends (differences between 2080–2100 and 1995–2014) in DJF and JJA

WB components	AMZ	LPB	ME	EA
GCMs (RegCM4) Reference Period – DJF				
P	8.5 (6.5)	6.0 (5.6)	2.7 (1.8)	1.9 (1.6)
ET	4.2 (4.1)	4.7 (4.2)	0.8 (0.6)	0.5 (0.5)
C	3.7 (2.2)	1.4 (0.8)	2.3 (2.4)	1.3 (0.6)
P-ET-C	0.6 (0.2)	– 0.1 (0.6)	– 0.4 (– 1.2)	0.1 (0.5)
GCMs (RegCM4) trends (future minus reference) – DJF				
P	– 0.5 (– 0.5)	0.3 (0.6)	0.6 (0.5)	0.5 (0.3)
ET	– 0.2 (0.0)	– 0.2 (0.1)	0.2 (0.1)	0.1 (0.2)
C	– 0.4 (– 0.3)	0.5 (0.7)	0.5 (0.8)	0.1 (0.1)
P-ET-C	0.1 (– 0.2)	0.0 (– 0.2)	– 0.1 (– 0.4)	0.3 (0.0)
GCMs (RegCM4) Reference Period – JJA				
P	1.3 (1.1)	1.7 (1.4)	2.2 (2.3)	2.0 (1.9)
ET	3.0 (2.4)	1.5 (1.5)	2.8 (3.0)	3.0 (2.6)
C	– 1.4 (– 1.0)	1.2 (– 0.5)	– 0.5 (– 0.3)	– 0.5 (– 1.4)
P-ET-C	– 0.3 (– 0.3)	– 1.0 (0.4)	– 0.1 (– 0.4)	– 0.5 (0.7)
GCMs (RegCM4) trends (future minus reference) – JJA				
P	– 0.1 (– 0.4)	0.0 (0.0)	– 0.8 (– 0.2)	– 0.7 (– 0.1)
ET	– 0.4 (– 0.7)	– 0.1 (0.0)	– 0.4 (0.0)	– 0.6 (0.0)
C	0.9 (0.3)	0.3 (– 0.1)	– 0.6 (– 0.2)	0.0 (– 0.4)
P-ET-C	– 0.6 (0.0)	– 0.2 (0.1)	0.2 (0.0)	– 0.1 (0.3)

Units: mm day^{-1}

Table 4 Slope of the linear regression model between trends of precipitation and evapotranspiration (P, ET), and precipitation and convergence (P, C), depicted in the trimesters DJF and JJA for each region

	DJF		JJA	
Region	P, ET	P, C	P, ET	P, C
AMZ	0.22 (0.09)	0.58 (0.30)	1.70 (1.50)	– 3.50 (– 0.63)
LPB	– 0.23 (0.08)	1.40 (0.98)	– 0.10 (0.42)	2.70 (0.00*)
ME	0.29 (0.18)	0.78 (1.43)	0.48 (-0.33)	0.82 (0.44)
EA	0.46 (0.36)	0.38 (0.11)	0.88 (0.52)	– 0.08 (1.00)

Global (RegCM4) values are shown outside (inside) the parenthesis. All slopes present p value < 0.05 except when marked with*

projections over the ME region (Fig. 4k). Consequently, for this region, the residual term is higher in the RegCM4 ensemble than in the GCMs (Fig. 4l). Note that the regional model has a great potential to substantially modulate the driving GCM signals in these relatively small regions placed far away from the domain's boundaries (e.g. RegCM4 MPI-ESM-LR). For both ME and EA regions the residual trend is smaller than the precipitation change signal (Table 3). Therefore, the increase of ET stands as the main driver of the precipitation change signal over the EA, which presents high slope for both ensembles (Table 4). In the ME region, the comparison of slope coefficients indicates that the precipitation change signal is mostly driven by the moisture flux convergence (Table 4).

During JJA (Fig. 5), over the AMZ the precipitation in both the global and regional projections progressively decreases throughout the century (Fig. 5a). This decline is mainly linked to a corresponding ET decrease (Fig. 5b). On the other hand, most of global and regional projections show an increment in moisture flux convergence (Fig. 5c), especially after 2050, indicating that the large-scale atmospheric moisture transport is not the main driver of the precipitation decline. Rather, the ET signal might point to be of greater relevance due to local P-ET feedbacks, as also indicated by the strong slopes in both P and ET, as shown in Table 4. In this case, it is important to highlight the added value of RegCM4 in reducing the moisture flux convergence of HadGEM2-ES, which stands out in comparison to the other projections (see the reduced slope in RegCM4 with respect to the GCM in Table 4). As the tropical Atlantic moisture transported to AMZ in JJA is lower than in DJF, it is expected that the ET exerts a greater influence on precipitation. Only the regional ensemble presents changes in ET and P larger than the residual term (Table 3), which supports the previous arguments. Over the AMZ, GCMs have a change in the residual term of ~ – 0.6 mm day^{-1}, which is higher than the difference of precipitation between the future and reference periods (– 0.1 mm day^{-1}; Table 4). This does not allow us to identify which mechanism drives the JJA precipitation change signal for the end of the century in AMZ for the GCMs.

In LPB (Fig. 5e–h), the precipitation barely changes until around 2060, after which the global ensemble projects an increase with respect to the reference of less than 0.2 mm day^{-1} and the regional ensemble a smaller increase around 0.1 mm day^{-1} later in the century. In the global model ensemble, the moisture flux convergence would be the main driver of precipitation changes, as suggested by the slopes of the regression curves, while the ET is the main driver for the regional model ensemble (Table 4). Precipitation over the LPB is mainly associated with transient synoptic system (Reboita et al. 2010; de Jesus et al. 2016) and both the global and regional models have systematic underestimation errors

Journal : Large 382 | Article No : 5539 | Pages : 14 | MS Code : 5539 | Dispatch : 21-11-2020

in representing these systems (de Jesus et al. 2016; Llopart et al. 2020), which might explain the residual term exceeding the precipitation change signal at the end of the century (see Fig. 5h and Table 3). Also in this case, as the residual is higher than the precipitation change signal it is difficult to separate which component drives the precipitation changes.

Analysis of the JJA water budget over the two European regions offers some interesting considerations (Fig. 5i–p). In all GCM simulations, we find a general decrease of moisture flux convergence over the ME region throughout the century (Fig. 5k). However, while this clearly drives a corresponding decrease of precipitation and ET in the global models, it is not reflected in corresponding trends in the RegCM4 simulations (Fig. 5i, j). Rather, precipitation shows a much less pronounced reduction, while the ET anomalies exhibit either some oscillations or even a small increase over both European domains. In contrast, over the EA the GCM ensemble shows a moisture flux convergence increase by the end of the century, which instead decreases in the RegCM4 ensemble (Fig. 5o). Therefore, in EA the precipitation change signal in the regional and global projections indicate different driving mechanisms (Tables 3 and 4). In the GCMs the residual term is smaller than the precipitation decrease and this decrease is explained mainly by a reduction in ET (slopes in Table 4). Conversely, in the regional model projections the residual exceeds the precipitation trend, making difficult to isolate what process is controlling the precipitation trends, although the ET appears to still have an important role. One factor in this difference, can be the higher resolution topography, which has already been shown to modulate the boreal summer precipitation change signal through high elevation heating and resulting convection (Figure S3, Giorgi et al. 2016; Torma and Giorgi 2020).

In the analysis, it is important to point out that the residual of the atmospheric water balance equation can have the same order of magnitude as the other terms during a warming period, because of the increasing water holding capacity of warmer air and possible changes in relative humidity. In fact, a relatively large residual term in Table 3 is seen for JJA in the GCMs (AMZ and LPB) and RegCM4 (LPB and EA), making it difficult to identify which component drives the changes in precipitation.

For DJF, the residual term is much smaller than the changes in precipitation in both the global and regional ensembles. For the AMZ region, the GCM and RegCM4 ensembles show a decrease in ET and C, i.e., both contribute to the precipitation change signal (with a higher contribution of C). This implies that remote processes are the main drivers of the precipitation change signal, associated with a weakening of the trade winds (Fig. 2a, b). On the other hand, in JJA over the AMZ, the reduction of precipitation projected by RegCM4 (~ $-$ 0.4 mm day^{-1}) is linked to a decrease in ET (~ $-$ 0.7 mm day^{-1}) indicating that local feedbacks are dominant in driving the precipitation change signal. Regarding the LPB region, for DJF, the main driver of the precipitation change at the end of the century is the moisture flux convergence from the Southern Atlantic Ocean, i.e. a remote process dominates the change signal (Fig. 2a, b; Table 4).

Over the ME, the increase (decrease) in precipitation during DJF (JJA) can be linked to both components of the atmospheric water balance, with a higher contribution of C than ET (Table 3). This means that the moisture flux convergence (divergence) is the main driver of the precipitation change signal (Figs. 2 and 3). Over the EA region, during DJF there is a prevailing effect of local feedbacks, i.e., ET drives the increase in precipitation in the RegCM4 ensemble (Table 4).

4 Conclusions

In this study, the atmospheric water budget is used to assess the sources of the future climate precipitation change signal over South America and Europe in an ensemble of CORDEX-CORE simulations. In particular, we focus on the Amazon (AMZ), La Plata basin (LPB), Mid-Europe (ME) and Eastern Europe (EA) regions in an ensemble of twenty-first century projections (from 1970 to 2100) of five RegCM4 simulations under the RCP8.5 scenario driven by four GCMs (MPI-ESM-MR, MPI-ESM-LR, NorESM1-M and HadGEM2-ES).

In general, the precipitation changes for DJF and JJA over both domains are in agreement with previous studies (Sánchez et al. 2015; Llopart et al. 2020; Christensen and Christensen 2007; Giorgi and Lionello 2008; Jacob et al. 2014, 2020). Over the SAM, there is a dipole pattern of change in precipitation, i.e. drier conditions in the northern regions and wetter conditions in central-eastern parts of the continent, which can be associated with changes in the circulation pattern at 850 hPa. Over Europe, the precipitation change signal shows a strong seasonality, i.e. during DJF (JJA) the projections indicate wet (dry) conditions, while in SAM this seasonality is not found. Over the European subdomains, the projected changes in precipitation, following Giorgi and Lionello (2008), might be attributed to the seasonal northward migration of the mid-latitude storms track.

The evaluation of the atmospheric water budget for the reference period shows that during the summer (DJF in SA and JJA in Europe) the evapotranspiration stands out as the main feature controlling precipitation in all subdomains. While in SAM the moisture flux convergence adds a contribution to the precipitation, in Europe it acts in the opposite direction, since moisture flux divergence predominates. In winter (JJA in SA and DJF in Europe), the moisture flux convergence is the main driver of precipitation for the European

Journal : Large 382	Article No : 5539	Pages : 14	MS Code : 5539	Dispatch : 21-11-2020

subdomains, while evapotranspiration continues be the main driver for the SAM subdomains.

Focusing on the changes in the selected subdomains, the spread among the ensemble members for precipitation is largest after 2050 and during the rainy seasons. According to the atmospheric water budget, during the boreal winter the precipitation change signals in the European subregions are controlled by the changes of both large-scale moisture flux convergence (most important in ME) and evapotranspiration (most important in EA). In EA during boreal summer the climate change signals of the water budget terms are different between the GCM and RegCM4 ensembles, making it difficult to conclude what process is controlling the precipitation changes. Over SAM, the evapotranspiration and moisture flux convergence change signals are not necessarily the same, and consistent with the precipitation changes, depending on region and season.

The global and regional model ensembles indicate an increase of precipitation in the LPB, mainly in DJF (11%), due to remote forcings, i.e., an increase in moisture convergence transported from the South Atlantic Ocean. During the austral summer, the LPB region has a strong land-surface feedback (hotspot) in present climate conditions (Sörensson et al. 2010; Sörensson and Menéndez 2011). Therefore, our result suggest that this hotspot tends to be reduced in future climate conditions, which agrees with previous studies (Ruscica et al. 2016).

The projections show a precipitation decrease over the AMZ, more pronounced in the RegCM4 ensemble than in the GCMs, mainly in JJA (− 40%). In this season, the precipitation decrease is associated with a reduction in evapotranspiration, which may imply that in the future the AMZ might become a hotspot for land-surface feedback during the austral winter. For DJF, moisture flux convergence is the main driver of the precipitation change signal in the AMZ and LPB, while for the ME region the opposite is projected to occur, i.e., ET drives the precipitation change signal.

The residual term in the atmospheric water budget is an important feature to be considered in our analysis. In most cases, the precipitation change signal is greater than the residual term, and in these cases the water budget approach provides a great potential to improve understanding of the mechanisms controlling the precipitation change signal. However, in a few cases (GCMs in AMZ and LPB, RegCM4 in LPB and EA, all in JJA) the residual term is greater than the precipitation change term and therefore it does not allow us to conclude what is driving the precipitation changes. This may be due to the parameterizations of convection and land surface schemes, but also to an increase in tropospheric specific humidity in response to a greater water holding capacity in warmer conditions.

Our results indicate that different driving processes related to the atmospheric and surface water budgets may be the main controls of precipitation change. This has important implications for modeling and understanding regional precipitation changes, since in cases where local rather than large scale atmospheric drivers dominate, the use of different physical schemes in the models can add another level of uncertainty.

Acknowledgements This paper was supported by the János Bolyai Research Scholarship of the Hungarian Academy of Sciences, Coordenação de Aperfeiçoamento de Pessoal de Nível Superior (CAPES, Brazil) Finance Code 001 and Conselho Nacional de Desenvolvimento Científico e Tecnológico—Brazil (CNPq, 422042/2018-8 and 420262/2018-0). Lincoln Muniz Alves acknowledges support from the Newton Fund through the Met Office Climate Science for Service Partnership Brazil (CSSP Brazil), the DFG/FAPESP (Grant No. IRTG 1740/TRP 2011/50151-0, and 2015/50122-0), and the National Institute of Science and Technology for Climate Change Phase 2 under CNPq Grant (465501/2014-1). All data from SAM-CORDEX and EURO-CORDEX modelling groups used in this work are acknowledged. The data used in this work can be found at the following web site: http://cordexesg.dmi.dk/esgf-web-fe/. We thank the reviewers for their constructive and helpful comments and suggestions.

References

Ambrizzi T, Reboita MS, da Rocha RP, Llopart M (2019) The state of the art and fundamental aspects of regional climate modeling in South America. Ann NY Acad Sci 1436:98–120

Ashfaq M, Cavazos T, Reboita MS et al (2020) Robust late twenty-first century shift in the regional monsoons in RegCM-CORDEX simulations. Clim Dyn. https://doi.org/10.1007/s00382-020-05306-2

Bentsen BI, Debernard JB, Iversen T, Kirkevåg A, Seland Ø, Drange H, Roelandt C, Seierstad IA, Hoose C, Kristjánsson JE (2012) The Norwegian Earth System Model, NorESM1-M. Part 1: description and basic evaluation. Geosci Model Dev Discuss 5:2843–2931

Blázquez J, Solman SA (2019) Relationship between projected changes in precipitation and fronts in the austral winter of the Southern Hemisphere from a suite of CMIP5 models. Clim Dyn 52:5849–5860. https://doi.org/10.1007/s00382-018-4482-y

Boé J, Somot S, Corre L, Nabat P (2020) Large discrepancies in summer climate change over Europe as projected by global and regional climate models: causes and consequences. Clim Dyn 54:2981–3002

Brêda JPLF, de Paiva RCD, Collischon W et al (2020) Climate change impacts on South American water balance from a continental-scale hydrological model driven by CMIP5 projections. Clim Change. https://doi.org/10.1007/s10584-020-02667-9

Brönnimann S, Xoplaki E, Casty C et al (2007) ENSO influence on Europe during the last centuries. Clim Dyn 28:181–197. https://doi.org/10.1007/s00382-006-0175-z

Brubaker KL, Entekhabi D, Eagleson PS (1993) Estimation of continental precipitation recycling. J Clim 6(6):1077–1089

Brutsaert W (2008) Hydrology: an introduction. 3rd ed. Hydrology: an introduction

Chou S, Lyra A, Mourão C et al (2014) Evaluation of the eta simulations nested in three global climate models. Am J Clim Change 3:438–454

Christensen JH et al (2007) Regional climate projections. In: Solomon S et al (eds) Climate change 2007: the physical science basis. Contribution of Working Group I to the Fourth Assessment Report of the Intergovernmental Panel on Climate Change. Cambridge University Press, Cambridge, pp 847–940

Christensen JH, Christensen OB (2007) A summary of the PRUDENCE model projections of changes in European climate by the end of this century. Clim Change 81:7–30. https://doi.org/10.1007/s10584-006-9210-7

Christensen JH, Boberg F, Christensen OB, Lucas-Picher P (2008) On the need for bias correction of regional climate change projections of temperature and precipitation. Geophys Res Lett 35:L20709. https://doi.org/10.1029/2008GL035694

Ciarló JM, Coppola E, Fantini A et al (2020) A new spatially distributed added value index for regional climate models: the EURO-CORDEX and the CORDEX-CORE highest resolution ensembles. Clim Dyn. https://doi.org/10.1007/s00382-020-05400-5

Ciarlo` JM, Fantini A, Stocchi P (2018) An Overview of EURO-CORDEX Simulations using RegCM4. In: Ninth ICTP Workshop on Theory and Use of Regional Climate Models, http://indico.ictp.it/event/8313/session/0/contribution/6/material/slides/0.pdf

Coppola E, Giorgi F (2010) An assessment of temperature and precipitation change projections over Italy from recent global and regional climate model simulations. Int J Climatol 30:11–32

da Rocha RP, Reboita MS, Dutra LMM, Llopart MP, Coppola E (2014) Interannual variability associated with ENSO: present and future climate projections of RegCM4 for South America-CORDEX domain. Clim change 125(1):95–109

de Jesus EM, da Rocha RP, Reboita MS, Llopart M, Mosso Dutra LM, Remedio ARC (2016) Contribution of cold fronts to seasonal rainfall in simulations over the southern La Plata Basin. Clim Res 68:243–255. https://doi.org/10.3354/cr01358

Dezsi Ş, Mîndrescu M, Petrea D, Rai PK, Hamann A, Nistor M-M (2018) High resolution projections of evapotranspiration and water availability for Europe under climate change. Int J Climatol 38:3832–3841. https://doi.org/10.1002/joc.5537

Dirmeyer PA, Fang G, Wang Z, Yadav P, Milton AD (2014) Climate change and sectors of the surface water cycle in CMIP5 projections. Hydrol Earth Syst Sci Discuss 11:8537–8569

Drumond A, Nieto R, Gimeno L, Ambrizzi T (2008) A Lagrangian identification of major sources of moisture over Central Brazil and La Plata Basin. J Geophys Res Atmos 113 (D14)

Furusho-Percot C, Goergen K, Hartick C, Kulkarni K, Keune J, Kollet S (2019) Pan-European groundwater to atmosphere terrestrial systems climatology from a physically consistent simulation. Sci Data 6:320

Giorgetta M, Jungclaus J, Reick C et al (2012) CMIP5 simulations of the Max Planck Institute for Meteorology (MPI-M) based on the MPI-ESM-LR model: The rcp85 experiment, served by ESGF. World Data Cent Clim

Giorgi F (2019) Thirty years of regional climate modeling: where are we and where are we going next? J Geophys Res Atmos 124:5696–5723. https://doi.org/10.1029/2018JD030094

Giorgi F, Coppola E (2007) European climate-change oscillation (ECO): 2007. Geophys Res Lett 34:L21703. https://doi.org/10.1029/2007GL031223

Giorgi F, Coppola E (2009) Projections of twenty-first century climate over Europe. Eur Phys J Conf 1:29–46

Giorgi F, Lionello P (2008) Climate change projections for the Mediterranean region. Global Planet Change 63:90–14 AQ2

Giorgi F, Jones C, Asrar G (2009) Addressing climate information needs at the regional level: the CORDEX framework. WMO Bull 58:175–183

Giorgi F, Coppola E, Solmon F et al (2012) RegCM4: model description and preliminary tests over multiple CORDEX domains. Clim Res 52:7–29

Giorgi F, Torma C, Coppola E, Ban N, Schär C, Somot S (2016) Enhanced summer convective rain at Alpine high elevations in response to climate warming. Nat Geosci 9:584–589. https://doi.org/10.1038/ngeo2761

Grønås S (1995) The seclusion intensification of the New Year's Day storm 1992. Tellus A 47:733–746. https://doi.org/10.3402/tellusa.v65i0.19539

Gutowski WJ Jr, Giorgi F, Timbal B, Frigon A, Jacob D, Kang H-S, Raghavan K, Lee B, Lennard C, Nikulin G, O'Rourke E, Rixen M, Solman S, Stephenson T, Tangang F (2016) WCRP COordinated Regional Downscaling EXperiment (CORDEX): a diagnostic MIP for CMIP6. Geosci. Model Dev. 9:4087–4095. https://doi.org/10.5194/gmd-9-6914087-2016

Held I, Soden B (2006) Robust responses of the hydrological cycle to global warming. J Clim 19(21):5686–5699. https://doi.org/10.1175/JCLI3990.1

IPCC (2013) Climate Change 2013: The Physical Science Basis. Contribution of Working Group I to the Fifth Assessment Report of the Intergovernmental Panel on Climate Change [Stocker, T.F., D. Qin, G.-K. Plattner, M. Tignor, S.K. Allen, J. Boschung, A. Nauels, Y. Xia, V. Bex and P.M. Midgley (eds.)]. Cambridge University Press, Cambridge, United Kingdom and New York, NY, USA, 1535 pp, https://doi.org/10.1017/CBO9781107415324

Jacob D, Petersen J, Eggert B et al (2014) EURO-CORDEX: new high-resolution climate change projections for European impact research. Reg Environ Change 14:563–578. https://doi.org/10.1007/s10113-013-0499-2

Jacob D, Kotova L, Teichmann C, Sobolowski SP, Vautard R, Donnelly C, Koutroulis AG, Grillakis MG, Tsanis IK, Damm A, Sakalli A, van Vliet MTH (2018) Climate Impacts in Europe Under +1.5°C Global Warming. Earth's Future 6:264–285. https://doi.org/10.1002/2017EF000710

Jacob D, Teichmann C, Sobolowski S, Katragkou E, Anders I et al (2020) Regional climate downscaling over Europe: perspectives from the EURO-CORDEX community. Reg Env Change. https://doi.org/10.1007/s10113-020-016060-9

Jones CD, Hughes JK, Bellouin N et al (2011) The HadGEM2-ES implementation of CMIP5 centennial simulations. Geosci Model Dev 4:543–570

Kain JS, Fritsch JM (1990) A one-dimensional entraining/detraining plume model and its application in convective parameterization. J Atmos Sci 47:2784–2802

Kotlarski S, Bosshard T, Lüthi D, Pall P, Schär C (2012) Elevation gradients of European climate change in the regional climate model COSMO-CLM. Clim Change 112:189–215

Kotlarski S, Keuler K, Christensen OB, Colette A, Déqué M, Gobiet A, Goergen K, Jacob D, Lüthi D, van Meijgaard E, Nikulin G, Schär C, Teichmann C, Vautard R, Warrach-Sagi K, Wulfmeyer V (2014) Regional climate modelling on European scales: a joint standard evaluation of the EURO-CORDEX RCM ensemble. Geosci Model Dev 7:1297–1333. https://doi.org/10.5194/gmd-7-1297-2014

Kovats RS, Valentini R, Bouwer LM, Georgopoulou E, Jacob D, Martin E, Rounsevell M, Soussana JF (2014) Europe. In: Climate Change (2014): Impacts, Adaptation, and Vulnerability. Part B: Regional Aspects. Contribution of Working Group II to the Fifth Assessment Report of the Intergovernmental Panel on Climate Change [Barros, V.R., C.B. Field, D.J. Dokken, M.D. Mastrandrea, K.J. Mach, T.E. Bilir, M. Chatterjee, K.L. Ebi,Y.O. Estrada, R.C. Genova, B. Girma, E.S. Kissel, A.N. Levy, S. MacCracken, P.R. Mastrandrea, and L.L. White(eds.)]. Cambridge University Press, Cambridge, United Kingdom and New York, NY, USA, pp 1267–1326

Llopart M, Coppola E, Giorgi F, da Rocha RP, Cuadra SV (2014) Climate change impact on precipitation for the Amazon and La Plata basins. Clim Change 125(1):111–125

Llopart M, da Rocha RP, Reboita M, Cuadra S (2017) Sensitivity of simulated South America climate to the land surface schemes in RegCM4. Clim Dyn 49(11–12):3975–3987

Journal : Large 382	Article No : 5539	Pages : 14	MS Code : 5539	Dispatch : 21-11-2020

Llopart M, Reboita MS, da Rocha RP (2020) Assessment of multi-model climate projections of water resources over South America CORDEX domain. Clim Dyn 54:99–116. https://doi.org/10.1007/s00382-019-04990-z

Lu J, Cai M (2009) Seasonality of polar surface warming amplification in climate simulations. Geophys Res Lett 36:1–6

Marengo JA, Soares WR, Saulo C, Nicolini M (2004) Climatology of the Low-Level Jet east of the Andes as derived from the NCEP reanalyses. J Clim 17:2261–2280

Marengo JA, Chou SC, Kay G et al (2012) Development of regional future climate change scenarios in South America using the Eta CPTEC/HadCM3 climate change projections: climatology and regional analyses for the Amazon, São Francisco and the Paraná River basins. Clim Dyn 38:1829–1848. https://doi.org/10.1007/s00382-011-1155-5

Mariotti L, Coppola E, Sylla MB, Giorgi F, Piani C (2011) Regional climate model simulation of projected 21st century climate change over an all-Africa domain: comparison analysis of nested and driving model results. J Geophys Res 116:D15111

Meehl GA, Bony S (2011) Introduction to CMIP5. Clivar Exchanges 16(56):4–5

Menéndez CG, Zaninelli PG, Carril AF, Sánchez E (2016) Hydrological cycle, temperature, and land surface atmosphere interaction in the La Plata basin during summer: response to climate change. Clim Res 68(2–3):231–241

Montini TL, Jones C, Carvalho LMV (2019) The South American low-level jet: a new climatology, variability, and changes. J Geophys Res Atmos

Moss RH, Edmonds JA, Hibbard KA et al (2010) The next generation of scenarios for climate change research and assessment. Nature 463(7282):747

Nascimento M, Herdies DL, Oliveira de Souza D (2016) The South American water balance: the influence of low-level jets. J Clim 29(4):1429–1449

Oleson KW, Lawrence DM, Bonan GB, Drewniak B, Huang M, Koven CD, Levis S, Li F, Riley WJ, Subin ZM, Swenson SC, Thornton PE, Bozbiyik A, Fisher R, Kluzek E, Lamarque J-F, Lawrence PJ, Leung LR, Lipscomb W, Muszala S, Ricciuto DM, Sacks W, Sun Y, Tang J, Yang Z-L (2013) Technical Description of version 4.5 of the Community Land Model (CLM), Tech. rep., National Center for Atmospheric Research. https://doi.org/10.5065/D6RR1W7M

Palmer MA, Reidy Liermann CA, Nilsson C, Flörke M, Alcamo J, Lake PS, Bond N (2008) Climate change and the world's river basins: anticipating management options. Front Ecol Environ 6:81–89

Peixoto JP, Oort AH (1992) Physics of climate. American Institute of Physics, New York, p 1992

Reboita MS, Gan MA, da Rocha RP, Ambrizzi T (2010) Regimes de Precipitação na América do Sul: Uma Revisão Bibliográfica. Revista Brasileira de Meteorologia 25(2):185–204

Reboita MS, da Rocha RP, Dias CG, Ynoue RY (2014) Climate projections for South America: RegCM3 driven by HadCM3 and ECHAM5. Adv Meteorol 2014:17 ((**Article ID 376738**))

Reboita MS, Fernandez JPR, Pereira Llopart M, Porfirio da Rocha R, Albertani Pampuch L, Cruz FT (2014) Assessment of RegCM4.3 over the CORDEX South America domain: sensitivity analysis for physical parameterization schemes. Clim Res 60:215–234

Reboita MS, Reale M, da Rocha RP et al (2020) Future changes in the wintertime cyclonic activity over the CORDEX-CORE southern hemisphere domains in a multi-model approach. Clim Dyn. https://doi.org/10.1007/s00382-020-05317-z

Ruscica RC, Menéndez CG, Sörensson AA (2016) Land surface–atmosphere interaction in future South American climate using a multi-model ensemble. Atmos Sci Lett 17:141–147. https://doi.org/10.1002/asl.635

Sánchez E, Solman S, Remedio ARC et al (2015) Regional climate modelling in CLARIS-LPB: a concerted approach towards twenty first century projections of regional temperature and precipitation over South America. Clim Dyn 45:2193

Sines T, Coppola E, Giorgi F, Sitz L (2018) South America CORDEX project using RegCM. In: Ninth ICTP Workshop on Theory and Use of Regional Climate Models, http://indico.ictp.it/event/8313/session/2/contribution/9/material/slides/0.pdf

Solman SA (2016) Systematic temperature and precipitation biases in the CLARIS-LPB ensemble simulations over South America and possible implications for climate projections. Clim Res 68(2–3):117–136

Sörensson AA, Menéndez CG (2011) Summer soil-precipitation coupling in South America. Tellus Ser A Dyn Meteorol Oceanogr 63:56–68

Sörensson AA, Menéndez CG, Samuelsson P, Willén U, Hansson U (2010) Soil-precipitation feedbacks during the South American Monsoon as simulated by a regional climate model. Clim Change 98:429–447

Tiedtke M (1996) An extension of cloud-radiation parameterization in the ECMWF model: the representation of subgrid-scale variations of optical depth. Mon Weather Rev 124:745–750

Torma C, Giorgi F (2020) On the evidence of orographical modulation of regional fine scale precipitation change signals: the Carpathians. Atmos Sci Let. https://doi.org/10.1002/asl.967 ((**in press**))

Torma C, Giorgi F, Coppola E (2015) Added value of regional climate modeling over areas characterized by complex terrain-Precipitation over the Alps. J Geophys Res Atmos 120:3957–3972. https://doi.org/10.1002/2014JD022781

van Vuuren DP, Edmonds J, Kainuma M et al (2011) The representative concentration pathways: an overview. Clim Change 109(1–2):5. https://doi.org/10.1007/s10584-011-0148-z

Zaninelli PG, Menéndez CG, Falco M, López-Franca N, Carril AF (2019) Future hydroclimatological changes in South America based on an ensemble of regional climate models. Clim Dyn 52:819